

Determination of Relative Permeabilities on Heterogeneous Samples

Fabrice Pairoys¹, Guillaume Lenormand², and Roland Lenormand²

¹TotalEnergies, CSTJF, Avenue Larribau, 64018 Pau Cedex, France

²Cydarex, 130 rue du port, 44420 Mesquer, France

Abstract.

The purpose of this paper is to improve the numerical simulations of oil/water waterfloods used to determine the relative permeabilities. Even if the samples are the more homogeneous as possible, the saturation profiles always present fluctuations. In this study we discuss the different methods to account for the various sources of heterogeneity in the simulation of the waterflood: porosity, permeability, and capillary pressure. The goal is to be able to numerically reproduce the measured fluctuations of the saturation profiles. We first describe the experiments: imbibition at reservoir conditions on two composite samples with similar plugs: a Semi-dynamic method (close to Unsteady state) and a Steady state. Then we describe several methods to account for heterogeneity: permeability profiles using Kozeny-Carman and Timur leading to Pc profiles using the Leverett J -function, and the original method from Egermann to derive Pc local curves from the saturation profiles. The main result is that only the Egermann method is able to reproduce the experimental saturation profiles. This result is an improvement for quality control of the simulation. However, for the Steady state experiment, the relative permeabilities determined by history matching are very close to the ones determined by the standard homogeneous approach. This study leads to a general procedure to improve the simulations of relative permeability experiments.

1 Introduction

When performing SCAL experiments to determine relative permeabilities, there is a quest for homogeneous samples. But when dealing with carbonate rocks, this quest becomes extremely difficult to reach, whatever the methods used (CT images, miscible tracer tests, MICP...). When core homogeneity is proved, coreflooding experiments are really a reliable way to estimate the microscopic efficiency. Question arises when dealing with heterogeneous samples.

Several methods are used to select the most homogeneous samples. The most routine technique, used in almost all laboratories, is X-ray CT imaging. It helps in discarding the most heterogeneous rocks by highlighting the presence of vugs, fractures/fissures, laminations, and high permeability streaks. CT-scanning can be performed on as-received whole cores, in their liners but can also be performed in X-ray transparent core holders, under reservoir conditions. It generally works well on clastic rocks. For carbonate rocks, heterogeneity exists at multiple scales: CT imaging is not always a robust enough technique to ensure that relevant heterogeneity is captured. It is possible to visualize small-scale heterogeneities in carbonate samples as explained by Hicks *et al.* [1]: but what to do when all available samples have same heterogeneous characteristics?

Mini-permeametry can also be used to obtain permeability mapping. It deals with gas injection at the rock surface, using a probe pressed against the rock. When gas rate and pressure become stable, permeability can be

calculated from analytical solution described by Gogging *et al.* [2]. This convenient and powerful technique works well on consolidated sandstone rocks, to capture permeability layout, but starts failing when performed on carbonate rocks, despite it may provide a trend. It may put in evidence high heterogeneity as explained by Dauba *et al.* [3]. The method is also limited to permeability measurements at the near rock surface, the inner part of core remaining inaccessible.

Tracer test technique can be performed to identify longitudinal heterogeneities within a rock sample. This test is generally performed after rock cleaning, drying, and saturating the sample with formation brine. Brine/brine miscible displacement is then performed using a second brine of different salinity, by recording the brine density at the outlet. Diagnosis of heterogeneity can be derived from the shape of the elution curve as explained Dauba *et al.* [3]: a dispersive rock exhibits an early breakthrough and long tail of production. Miscible tracer tests should always be carried out before any waterflooding tests as an indicator of heterogeneity.

Note that the presence of heterogeneity may also be observed when performing a water-oil primary drainage, by monitoring the differential pressure as shown by Saltani *et al.* [4] and Pairoys *et al.* [5].

The effect of small-scale heterogeneity on relative permeability has been investigated by Hamon and Roy [6], experimentally and numerically. They confirmed the conclusions made by Ferreol and Corre [7] that reliable relative permeability can be obtained from across-bedding samples. Hamon and Roy [6] also concluded that reliable

* Corresponding author: roland.lenormand@cydarex.fr

relative permeability curves can be extracted from heterogeneous rock when capillary forces are negligible, as long as it does not generate strong saturation variations along the sample (confirming Sylte's and Mannseth observations [8]).

If the interpretation process of laboratory coreflooding experiments is well established on homogeneous porous media, some questions remain open when dealing with heterogeneous rock samples:

- Can we interpret the experimental coreflooding results obtained on heterogeneous samples with homogeneous relative permeability Kr approach with the sample considered as homogeneous?
- Can we establish a new Kr approach to reproduce the noisy saturation profiles?
- Is there a significant difference between homogeneous and heterogeneous approaches for Kr determination?

To try to answer these questions, two datasets from a study published in 2021 by Pairoys *et al.* [9] were used. Two water-oil imbibition tests on a carbonate rock (composite of two core plugs) were performed at reservoir conditions, using the semi-dynamic (SDM) and the Steady state (SS) method. We recall that the SDM for negative Pc consists in injecting only brine, like in Unsteady state method, but with a circulation of oil at the outlet. The Semi-dynamic method with only water injection is similar to an Unsteady state method, but with a better-defined outlet condition, injected water being flowing in the outlet endpiece filled with oil by circulation, necessary condition to impose Pc=0. In both SDM and SS cases, saturation profiles present significant local variations, proving the presence of small-scale heterogeneities. In this study, 1D X-ray attenuation technique was used to determine the porosity profile and to monitor the saturation profiles along the composite stacks during the two-phase flow.

The Kr curves are determined first using analytical interpretations that neglect capillary pressures and assume uniform saturation profiles. It is well known that these analytical interpretations are not accurate and cannot reproduce the capillary end effect. A more accurate determination is obtained by numerical simulation of the displacements. The Kr (and Pc) are determined by minimizing the difference between the experimental results and simulated ones (difference of pressure across the sample dP and oil production). This history matching is performed automatically using the commercial software CYDAR (www.cydarex.fr) that allows non-uniform initial saturation profile, porosity and permeability profiles and multiple capillary pressures along the sample, but with a unique set of relative permeabilities.

We have first tested a standard approach in two steps: estimate the permeability profile then the Pc profile using the Leverett J -function, that assumes that the capillary pressure is inversely proportional to the mean pore radius of the sample leading to a scaling with $\sqrt{\varphi/K}$, K being the permeability and, φ the porosity. Generally, this

relationship is used in primary drainage, to estimate the field capillary pressure from a measurement in laboratory. We will assume, that this relationship between Pc and the mean pore radius is still valid in imbibition.

1) The permeability profile is estimated using a simplified Kozeny-Carman model (Eq. 1), [10], [11]:

$$K_{i(K-C)} = \frac{\varphi_i^3 d_p^2}{180(1-\varphi)^2} \quad (1)$$

With $K_{i(K-C)}$ the Kozeny-Carman local permeability, φ_i the local porosity and dP the average particle diameter derived from the average porosity and permeability values from Table 1.

We also tested the calculation of the permeability profile using Timur equation based on the initial saturation as in reservoir studies (Timur [12]):

$$K_{i(Timur)} = \left(\frac{93\varphi_i^{2.2}}{Sw_i} \right)^2 \quad (2)$$

With $K_{i(Timur)}$ the Timur local permeability, φ_i the local porosity and Sw_i the local initial water saturation from X-ray attenuation technique.

2) In a second step, we calculated the local Pc curves using the standard Leverett J -function, a function available in the software and then run the numerical simulation, followed by an automatic history matching.

We also tested the original approach described by Egermann *et al.* [13], [14], from now called the Egermann method. In a first approach, it is assumed that local variations of pressure field in heterogeneous medium are much smaller than saturation variations. Consequently, local capillary pressure curves can be obtained from the measured local saturations and the simulated pressure profiles, these profiles being obtained after running a numerical interpretation considering homogeneous porous medium. This step is called the homogeneous simulation. Then, heterogeneous simulations are performed using these local Pc curves, and the porosity profiles. Use of permeability profiles derived from the porosity have also been tested to calculate the initial Pc profiles (K-C and Timur). This step is called the Egermann method.

In the last step, that we call "iteration", the Pc profiles calculated with the Egermann method are used to determine a new set of local capillary pressures curves, and new Kr curves are determined by optimization. This iteration was suggested in Egermann's publications, but not demonstrated.

During each step, a set of Kr curves is determined by optimization (history matching) of the pressure difference and oil production.

In this paper, we present the description of the samples and the experimental results. Then we apply the heterogeneous approach on the two types of experiments SDM and SS. For the SDM, there is no real improvement of the result at the opposite of the Steady state experiment

that leads to a very good fit for the saturation profiles. We finally try to explain the result.

2 Experimental Description

2.1 Rock and fluid properties

In their study, Pairoys *et al.* [9] selected a tight carbonate reservoir rock to perform a challenging SCAL program. A first coreflooding test consisted in performing a waterflood on a composite stack of two core plugs, using the semi-dynamic method (SDM). A second test was also performed on a stack of two core plugs but using the Steady state method (SS).

CT images of the core plugs did not show the presence of significant heterogeneities such as vugs or fractures, but presence of dense materials represented by the bright spots, as shown in Figure 1.

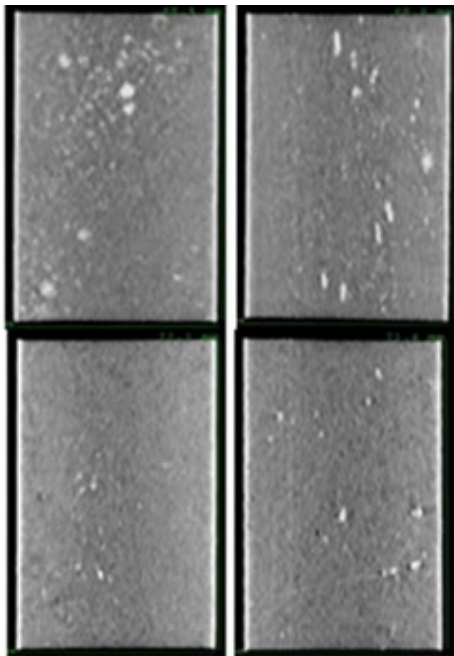


Fig. 1. CT images from the two SDM core plugs (top) and from the two SS core plugs (bottom).

Unfortunately, there were no miscible tracer (MTT) tests performed in this study. We recall that it is highly recommended to perform MTT to discard the rocks with too high longitudinal heterogeneity, especially for the unsteady state experiments.

When looking at the MICP result of an end-trim in Figure 2, a wide range of pore throat radius, varying from 0.03 micron to 3.5 microns, is observed.

It was also noticed in Pairoys *et al.* [9] that the rock had a certain degree of heterogeneity based on thin section (TS) and Scanning Electron Microscopy (SEM) observations, as shown in Figure 3.

All the above observations could indicate the presence of small-scale heterogeneities: it was confirmed by the porosity profiles of the two stacks, profiles measured with X-ray attenuation technique using the

reference scans obtained at the end of the experiments (Figure 4).

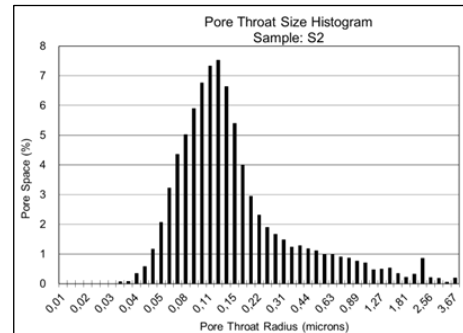


Fig. 2. MICP pore throat size distribution (PTSD) of 1 sample.

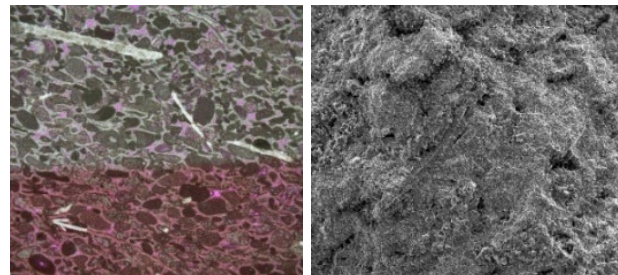


Fig. 3. Thin Section and SEM images.

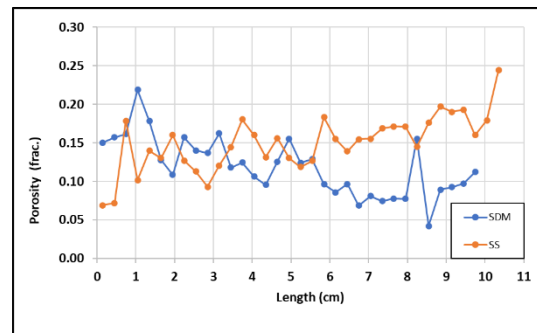


Fig. 4. Porosity profiles (SDM and SS).

Figure 4 confirms the heterogeneous character of the selected rock, with porosity spatially varying from 4.3% to 22.6% for the SDM stack, and from 6.9% to 24.4% for the SS stack. However, this porosity is measured along the X-ray beam and is not an average on the slice.

The dimensions, average porosity and brine permeability of the two stacks are provided in Table 1.

Table 1. Rock properties.

	Length (cm)	Diameter (cm)	Porosity ϕ (%)	Perm Kw (mD)
SDM	9.969	3.792	12.27	0.61
SS	10.524	3.806	14.97	1.30

Both experiments were performed in the same reservoir conditions (temperature of 100°C, pore pressure of 3,000 psi, confining pressure of 5,000 psi), using same

couple of fluids, doped brine and live oil. The fluid properties, at reservoir conditions, are listed in Table 2.

Brine and live oil were equilibrated to avoid any mass transfer.

Table 2. Fluid properties.

	Density ρ (g/cc)	Viscosity μ (cP)
Brine	1.11	0.48
Live oil	0.80	3.17

2.2 Experimental protocols

Two water-oil imbibition experiments using the SDM method and SS method respectively were performed at immiscible reservoir conditions, in vertical position, injection from bottom to top. The experimental setups are described by Pairoys *et al.* [9]: it included a differential pressure dP sensor, a visual separator to monitor the volume of oil produced and a 1D linear X-ray scanner to monitor the saturation profiles at 33 locations for SDM and 35 for SS (longer sample). For more details of the experimental protocol like core saturation, S_{wi} establishment, ageing, etc. it is referred to the original publication [9].

The X-ray saturation profiles at initial water saturation S_{wi} are shown in Figure 5.

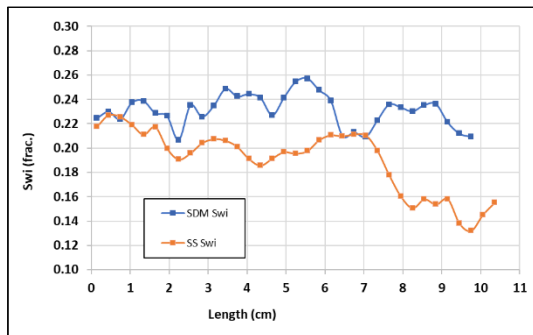


Fig. 5. SDM and SS S_{wi} profiles.

It can be noted that, despite all precautions taken to flatten the S_{wi} saturation profiles, significant local variations of saturation are observed. If the overall trend of the SS S_{wi} profile looks quite consistent with the observed porosity profile (increase in porosity with decrease in S_{wi} from left to right), it is less visible for the SDM case.

2.3 Experimental results: Semi-dynamic method

First, let's look at the SDM experimental dataset.

The equilibriums of the oil production (Figure 6) and differential pressure (Figure 7) at the end of each flow rates are not perfect, but acceptable, always difficult to reach well-defined equilibrium for experiments performed at reservoir conditions. However, numerical simulations allow interpretation even if the equilibrium is not completely reached.

As for porosity and S_{wi} profiles, spatial fluctuations of saturation at end of each step are observed.

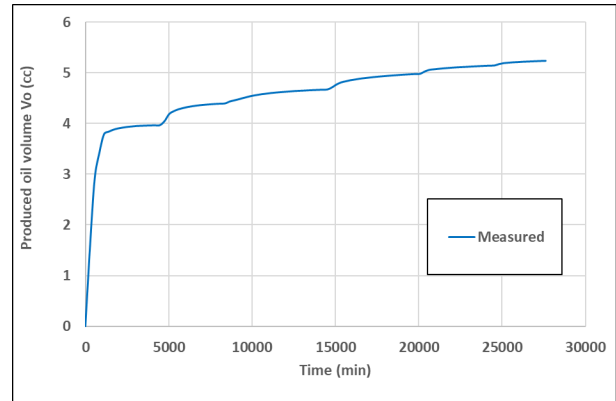


Fig. 6. SDM oil production versus time.

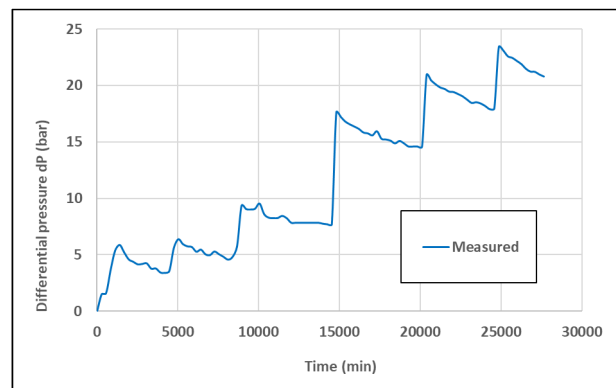


Fig. 7. SDM differential pressure versus time.

The saturation profiles at the end of each step are presented in Figure 8.

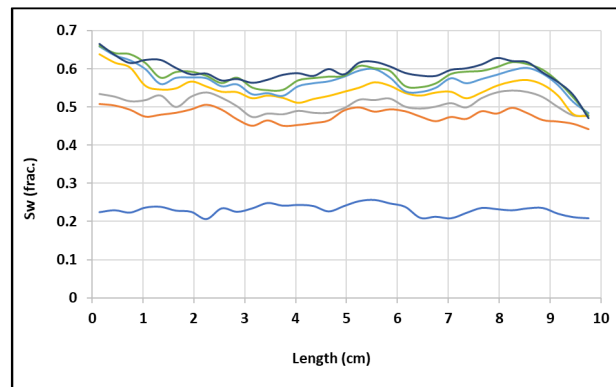


Fig. 8. SDM water saturation profiles, initial and at end of each step (from bottom to top).

2.4: Experimental results: Steady state method

Figure 9 and Figure 10 show acceptable equilibrium of oil production and differential pressure at the end of each ratio.

As for the SDM test, spatial variations of saturation at equilibrium are observed.

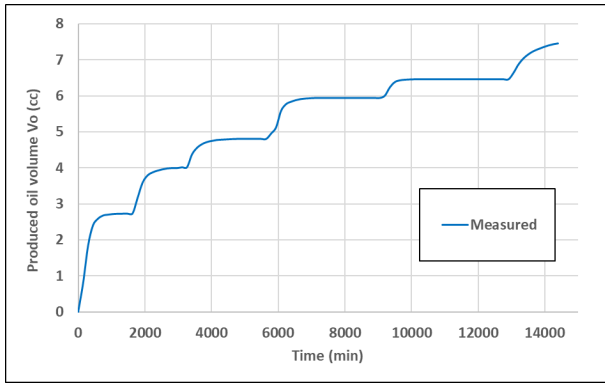


Fig. 9. SS oil production versus time.

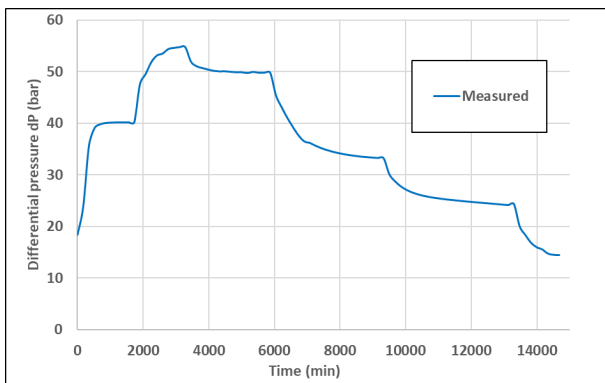


Fig. 10. SS differential pressure versus time.

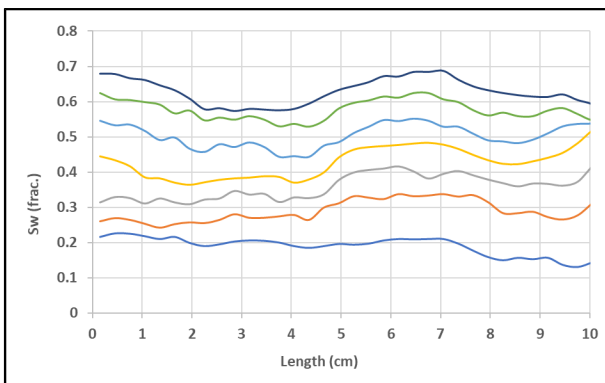


Fig. 11. SS water saturation profiles, initial and at end of each step (from bottom to top).

3 Interpretation of the SDM experiment

3.1 Homogeneous interpretation

The homogeneous approach consisted in history-matching the Corey relative permeability with the oil production and the dP signal. Since we will use permeability profiles, that are absolute permeability, it was preferable to use the absolute permeability as base perm for the simulations. The P_c curve, represented with a $\log(\text{Beta})$ function is adjusted “manually” to represent the capillary end effect on the saturation profiles.

The resulting K_r and P_c curves are presented in Figure 12, Figure 13 and table 4. For both analytical points and results of history matching, the results differ

from the values given in the original publication [9] due to differences in the base perm.

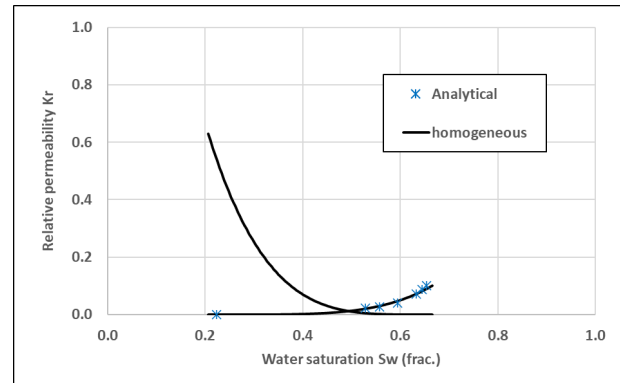


Fig. 12. SDM: History matched K_r curves using homogeneous approach (cartesian plot) and symbols from analytical calculation.

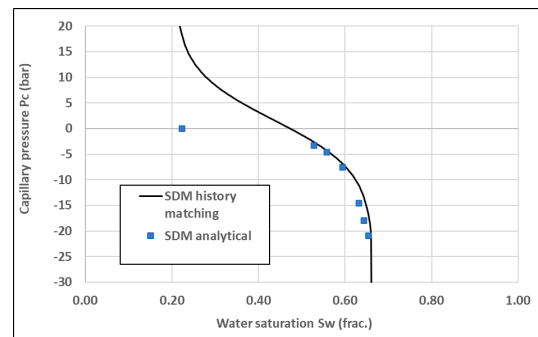


Fig. 13. SDM: History-matched P_c curves using homogeneous approach and values from analytical calculation.

The resulting parameters (Corey model and $\log\text{Beta}$ function) are listed in Table 4.

Table 4. K_r and P_c parameters ($K_{roMax}=0.63$ and $Sw_i=0.21$, P_o in bar) for the homogeneous interpretation of the SDM experiment.

N_w	N_o	K_{rwMax}	S_{or}	P_o	β	$Sw@P_c=0$
4.5	4.0	0.10	0.37	20	1.0	0.45

The history-match quality using homogeneous approach is shown in Figure 14, Figure 15, and Figure 16.

If the history-match quality of the oil production and dP signals (respectively Figure 14 and Figure 15) is acceptable, it is, as expected, not possible to history-match the experimental saturation profiles (Figure 16) using the homogeneous approach, except the initial profile that is used as input.

3.2 “Leverett J -Function” interpretation

As described in the introduction, we have first estimated a permeability profile using Kozeny-Carman and Timur approaches. All the permeabilities are normalized to agree with the measured value. Figure 17 shows that Timur values present more variations than Kozeny-Carman. In addition to the porosity profile, Timur uses the Sw_i profile that is also very noisy. That explains the difference between the two profiles.

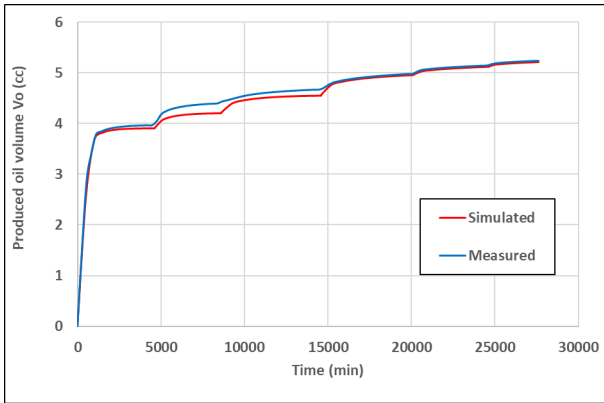


Fig. 14. SDM experimental versus simulated oil production with the homogeneous approach.

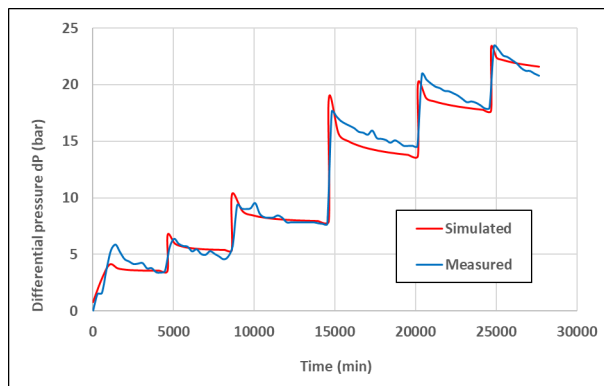


Fig. 15. SDM experimental versus simulated dP history-match with the homogeneous approach.

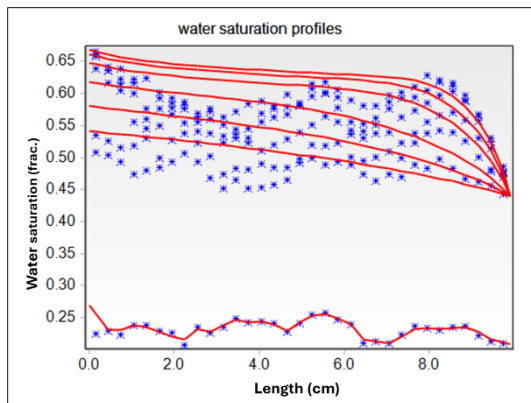


Fig. 16. SDM: Experimental (symbols) versus simulated (solid lines) saturation profiles with the homogeneous approach.

In a second step, we calculated the local P_c curves using the standard Leverett J -function and then run the numerical simulation, followed by an automatic history matching. The K-C case leads to saturation profiles that have just a tendency to represent the experiments (Figure 18). For the TIMUR case (Figure 19), the saturation profiles differ more from the experiment in the first part of the sample.

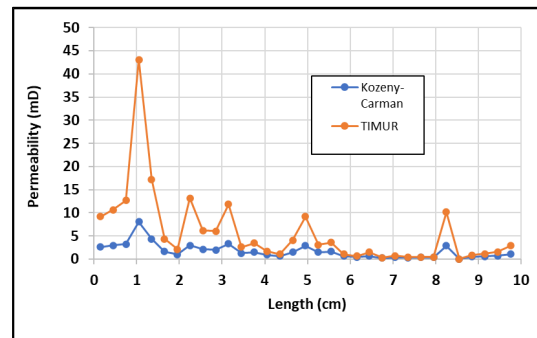


Fig. 17. SDM: Permeability profiles estimated with the Kozeny-Carman (K-C) and Timur approaches.

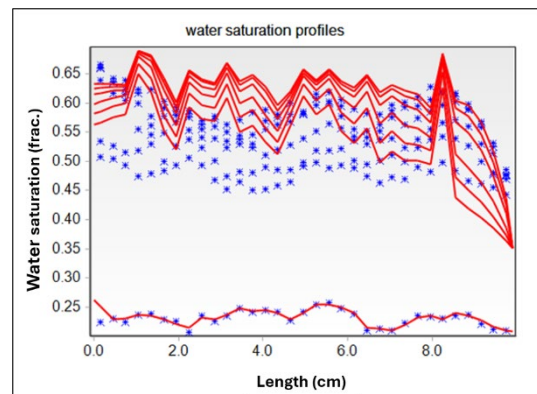


Fig. 18. SDM: Saturation profiles from the Leverett approach with the K-C permeability profile.

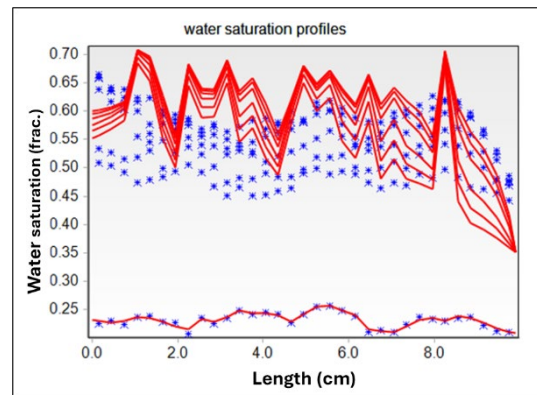


Fig. 19. SDM: Saturation profiles from the Leverett approach with the TIMUR permeability profile.

3.3 Egermann method

Using the Egermann method, 33 P_c curves were extracted from the P_c curves calculated at the same location than the X-ray locations, using the homogeneous approach (Figure 20) and saturation profiles at equilibrium at the same locations. The results are displayed in Figure 21, together with the average P_c curve determined from the homogeneous approach (in yellow).

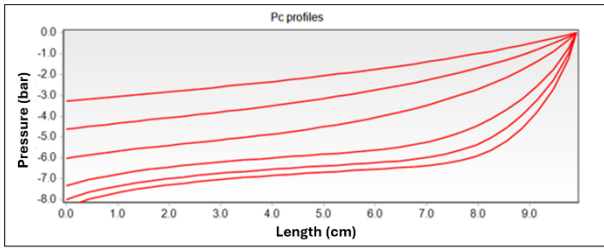


Fig. 20. SDM: Simulated capillary pressure profiles obtained from “homogeneous” approach.

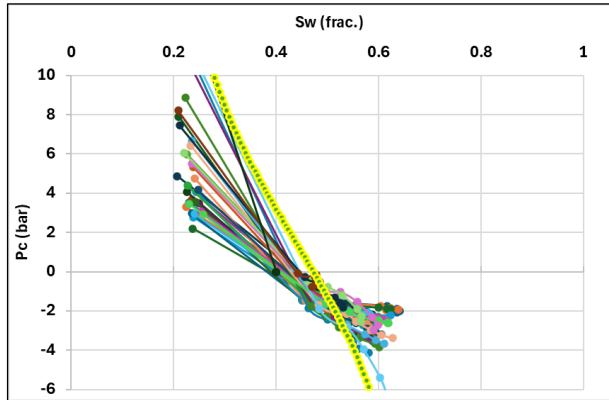


Fig. 21. SDM: The 33 local Pc calculated with the Egermann method and the Pc from homogeneous interpretation in yellow.

We first used these 33 local Pc curves for simulations with the porosity and K-C permeability profiles. The results (Figure 22) are similar to the profiles calculated with Leverett Pc curves (Figure 19), without the Egermann’s Pc curves.

With a constant permeability profile, the variation is less important (Figure 23).

From these two simulations, we can conclude that in this experiment, the effect of the K-C permeability profile is more important than the Pc profile.

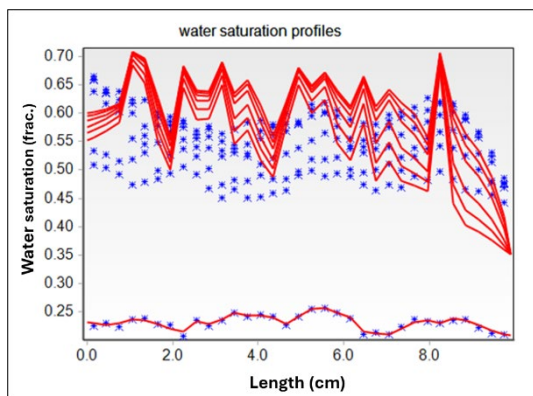


Fig. 22. SDM: Saturation profiles from the Egermann approach with the K-C permeability profile.

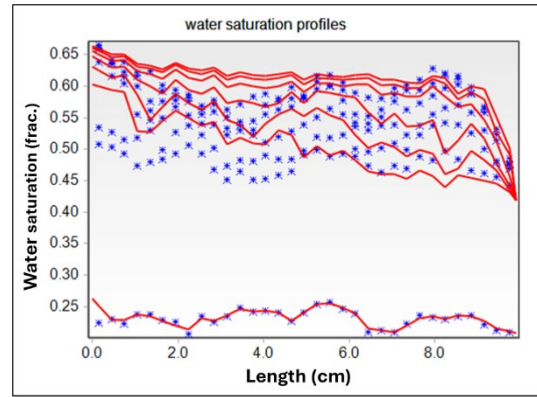


Fig. 23. SDM: Saturation profiles from the Egermann method with constant permeability profile.

The Kr curves differ slightly from the homogeneous case (Figure 24 and table 5) but there is no significant improvement for the fit of experiments (pressure and oil production), not shown here.

Table 5. Kr parameters for the interpretation of the SDM experiment with Egermann method (KroMax=0.62 and Swi=0.207).

Nw	No	KrwMax	Sor
3.5	4.2	0.08	0.34

We have also tested an iteration, as described in the introduction, using the capillary pressure profiles determined with the Egermann method as input for the calculation of a new set of local Pc curves, but there is no improvement.

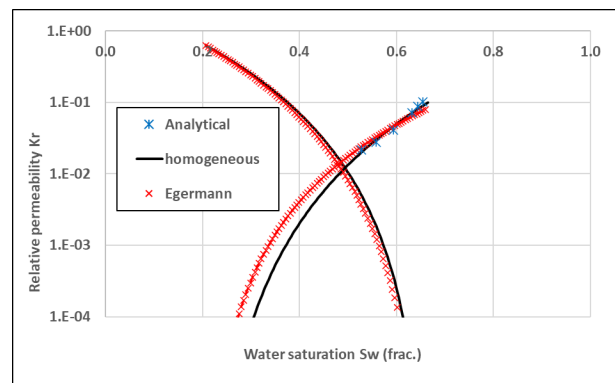
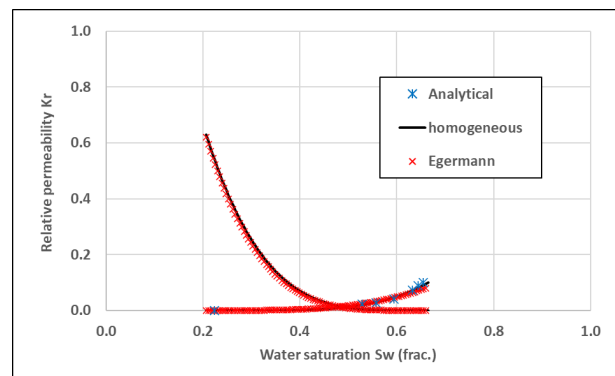


Fig. 24. Comparison between the SDM relative permeabilities: analytical, homogeneous and Egermann method (linear and logarithmic scales).

4 Interpretation of the SS experiment

We have followed the same approach as for the SDM experiment.

4.1 Homogeneous interpretation

Figure 25 and Figure 26 present the history-match of the experimental data with uniform porosity and permeability (homogeneous approach). For the oil production and dP the fit is not good: For most of the steps, the simulated transients are faster than the experimental ones. We have also tested more flexible functions. The modified Corey (two adjustable exponents instead of one for Corey) presents no improvement compared to Corey. The LET functions leads to non-physical shapes for the relative permeabilities and the results are not presented. We have no explanation for this difficulty to fit the experiments.

The resulting relative permeabilities are close to the analytical calculation (Figure 27 and Table 6). The SS P_c curve (Figure 28) is adjusted manually to fit the capillary end effect. This curve presents an important positive part, not determined in the SDM experiment.

The simulated saturation profiles follow the tendency of the experiments, but without reproducing the fluctuations, since it is a homogeneous approach (Figure 29).

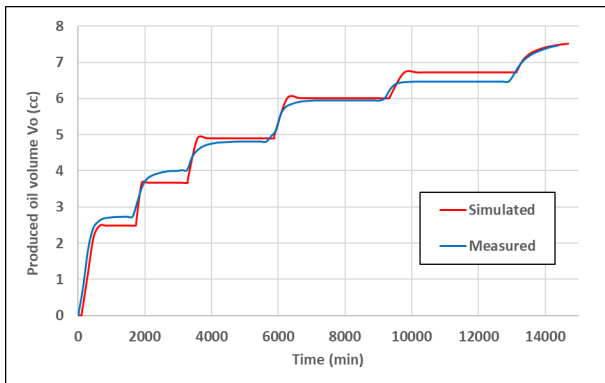


Fig. 25. SS: Experimental versus simulated oil production with the homogeneous approach.

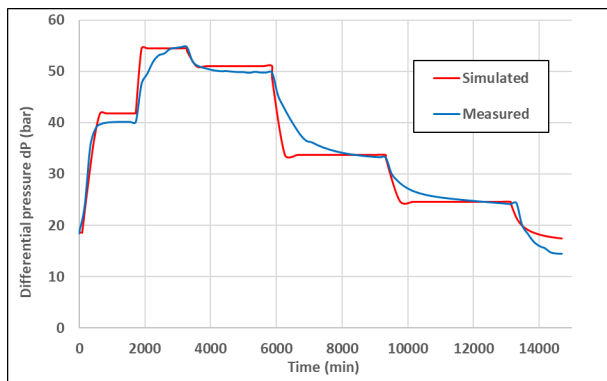


Fig. 26. SS: Experimental versus simulated dP history-match with the homogeneous approach.

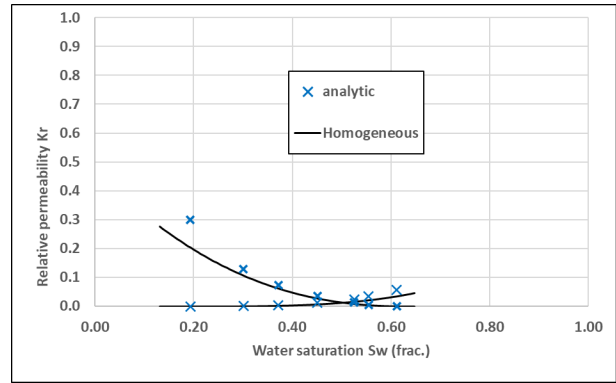


Fig. 27. SS: Relative permeabilities: analytical points and history matched curves using homogeneous approach.

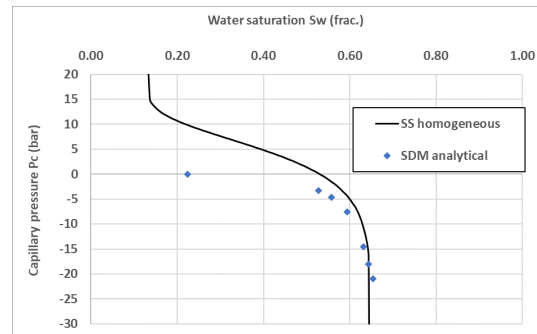


Fig. 28. History-matched SS P_c curves using homogeneous approach, compared to the points calculated analytically from the SDM experiment.

Table 6. K_r and P_c parameters for the homogeneous interpretation of the SS experiment ($K_{roMax}=0.276$ and $Sw_i=0.132$, P_o in bar).

N_w	N_o	K_{rwMax}	S_{or}	P_o	β	$Sw@Pc=0$
3.82	2.38	0.044	0.35	15	0.001	0.53

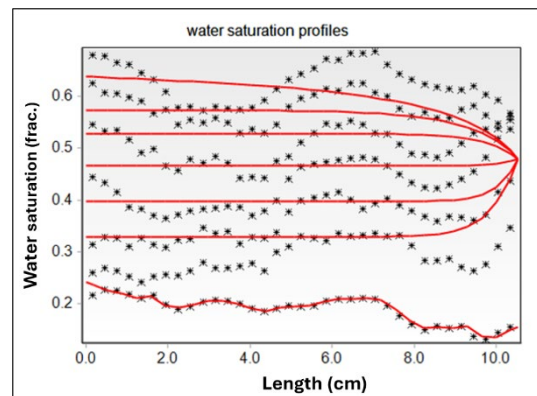


Fig. 29. SS: Saturation profiles from the homogeneous approach: Experimental (symbols) versus simulated (solid lines) saturation profiles.

The homogeneous interpretation is not able to reproduce the special fluctuations of saturation.

These fluctuations are due to the local heterogeneities, in porosity, permeability and capillary pressure. In order to study the respective role of these heterogeneities, we have first performed simulations with

uniform Pc (only porosity and permeability profiles) then with only the Pc profiles.

4.2 Uniform Pc interpretation with K-C permeability profile

As for the SDM experiment, we have first estimated a permeability profile using Kozeny-Carman and Timur approaches. All the permeabilities are normalized to agree with the measured value. Figure 30 shows that Timur values present more variations than Kozeny-Carman, probably due to the added heterogeneities on Swi.

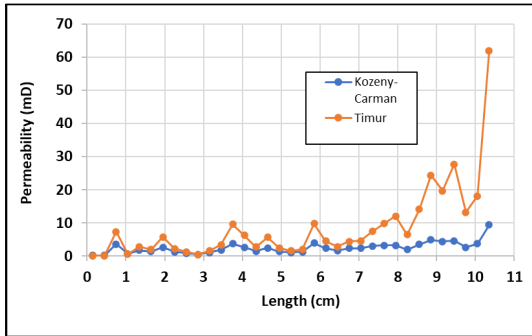


Fig. 30. SS: Permeability profiles estimated with the Kozeny-Carman (K-C) and Timur approaches.

We then calculated the saturation profiles with porosity and permeability profiles (K-C), but with uniform Pc (the same as for the homogeneous case). The result (Figure 31) is very similar to the homogeneous case (Figure 29). This result confirms the main assumption of the Egermann method: the local permeability variations are integrated along the sample and are not responsible for local saturation variations.

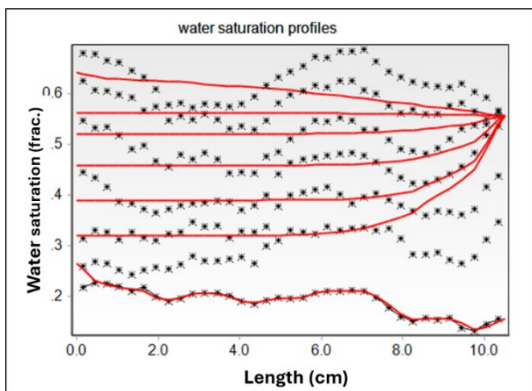


Fig. 31. SS: Saturation profiles with the K-C permeability profile and uniform Pc.

4.3 Leverett interpretation

The displacements are now simulated with local Pc curves derived with the Leverett *J*-function. We present only the results with K-C profiles that are better than TIMUR. The calculated saturation profiles follow the experiment trends but with less amplitude for the last steps (Figure 32).

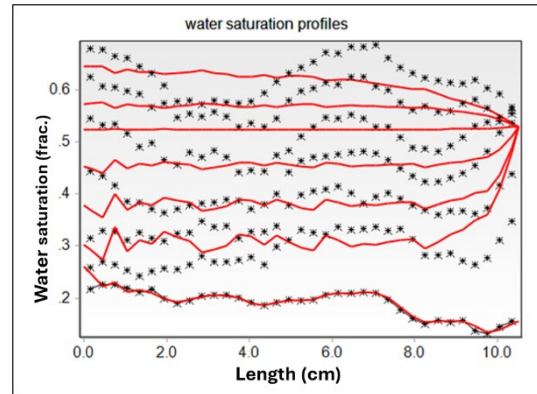


Fig. 32. SS: Saturation profiles from the Leverett approach with the K-C permeability profile

The relative permeabilities differ slightly from the homogeneous case (Figure 33) but there is no improvement of the history-match of the oil production and *dP*.

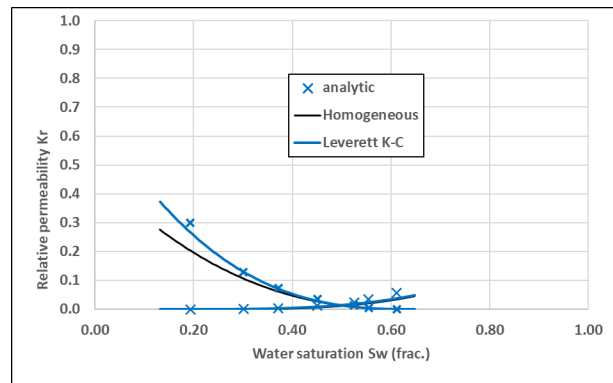


Fig. 33. Comparison between the SS relative permeabilities: analytical, homogeneous and Leverett approaches.

The Pc profiles are quite regular (Figure 34) except the one corresponding to Swi that is imposed (largest positive values).

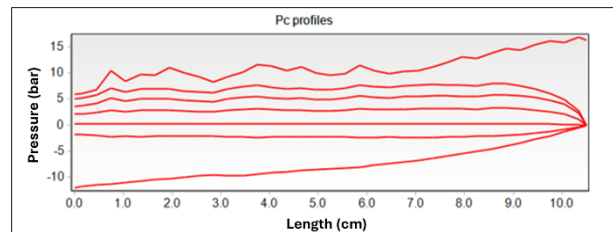


Fig. 34. SS: Simulated capillary pressure profiles obtained from the Leverett approach and used for the Egermann method.

4.3 Egermann method

For this experiment, we have used the Pc calculated with the Leverett approach (Figure 34) to calculate the 35 Pc curves since the saturation profiles are closer to the experimental ones than the homogeneous calculation. The results are displayed in Figure 35, together with the average Pc curve determined from the homogeneous approach (in yellow).

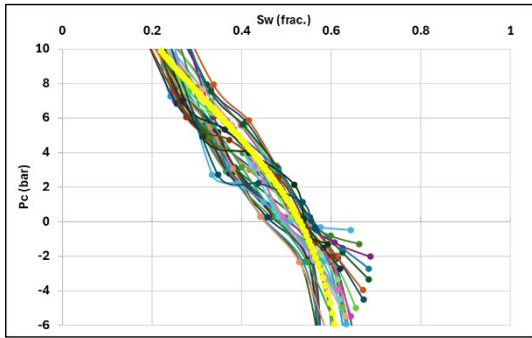


Fig. 35. SS: The 35 local Pc curves calculated from the Leverett Pc profiles. Homogeneous Pc in yellow.

The saturation profiles calculated with the Egermann Pc curves and the constant permeability profiles (Figure 36) are more in agreement with the experimental results than the Leverett ones (Figure 32), especially for the last steps. However, there is no improvement of the oil production and dP history-matching.

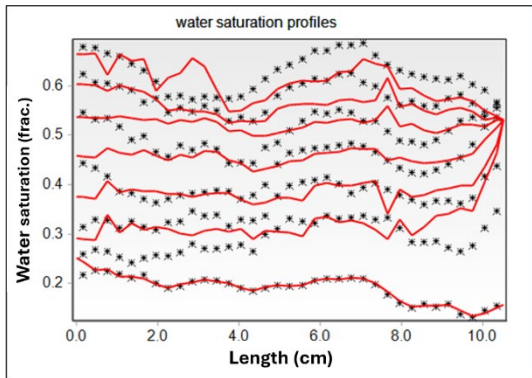


Fig. 36. SS saturation profiles from the Egermann method with the constant permeability profile.

4.4 Egermann method with iteration

As suggested by Egermann, we have tested an additional iteration step, using the Egermann Pc profile (Figure 37) as input for the determination of a new set of local Pc curves (Figure 38).

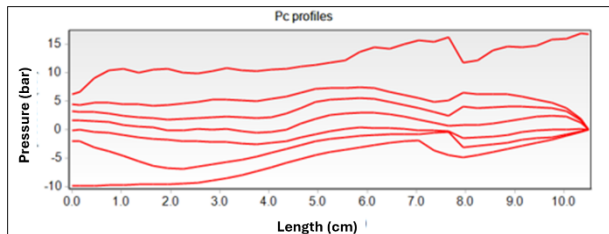


Fig. 37. SS simulated capillary pressure profiles obtained from the Egermann method and used for the iteration calculation.

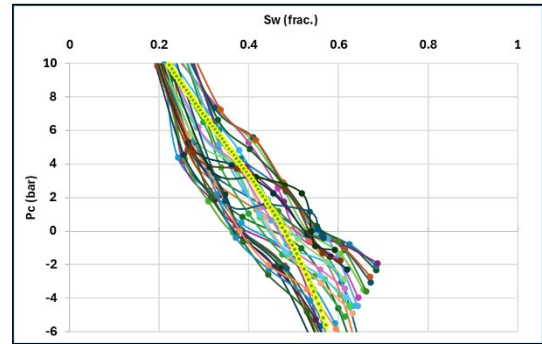


Fig. 38. SS Iteration. The 35 local Pc curves calculated from the Egermann Pc profiles. Homogeneous Pc in yellow

We have tested both K-C and constant permeability profiles to run the simulation, but always with the porosity profile. The constant permeability gives the best result for the saturation profiles (Figure 39) with a good agreement with the experiments.

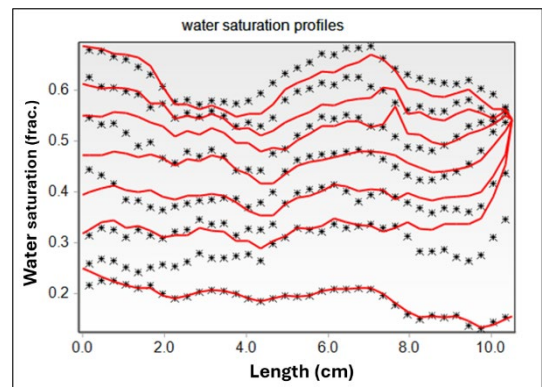


Fig. 39. SS: Saturation profiles from the Iteration method with the constant permeability profile.

The final relative permeabilities are very close to the ones determined with the homogeneous approach (Figure 40) and table 7. The curves are superimposed, except a small difference for the Sor (0.3 instead of 0.35). Therefore, the history-matches of oil production and dP are similar to the homogeneous case (Figure 25 and Figure 26).

Table 7. Kr parameters for the iteration interpretation of the SS experiment (KroMax=0.275 and Swi=0.132).

Nw	No	KrwMax	Sor
4.1	3.1	0.075	0.30

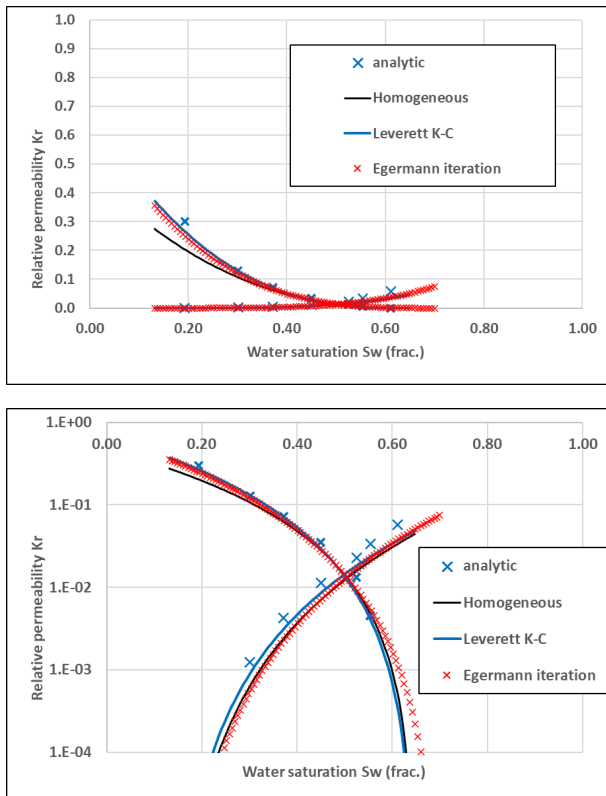


Fig. 40. Comparison between the SS relative permeabilities: analytical, homogeneous, Leverett and Egermann approaches (linear and logarithmic scales).

5 Discussion

In this study, our goal was to reproduce the fluctuations of the measured saturation profiles of oil/water waterfloods by numerical simulations.

We have used two experiments using SDM and SS methods presented in a previous SCA conference (Pairoy *et al.* [9]). In the original publication, the authors were not able to obtain a good fit between the experiments and the simulations. They used only a Corey model for the relative permeabilities. Even using more flexible functions (like LET), we were not able to improve the fits. We have no explanation for that. Using the provided data, and standard values for K_r and P_c leads to much faster equilibrium at each step. Consequently, we have focused our study on the saturation profiles that are of good quality.

There are several local variables that contribute to non-uniform saturation profiles: porosity, permeability, and capillary pressure. Only porosity and saturation profiles are measured directly with X-ray. The permeability profile can be derived either from porosity alone (Kozeny-Carman) or using the additional information on initial saturation (Timur).

In a first approach (for the SS experiment) we have shown that the porosity and permeability profiles alone were not able to reproduce the fluctuations of the saturation profiles. This result agrees with the results published by Egermann: local permeability fluctuations

are averaged due to the long-range correlation of the pressure field and do not contribute to saturation fluctuations.

In a second approach, we have used the porosity and permeability profiles to derive P_c profiles using the standard Leverett J -function. From both SDM and SS experiments, we have shown that this approach was not able to reproduce the amplitude of the measured saturation profiles. Why? The notion of correlations between porosity and permeability is well established in reservoir engineering (rock typing), but there is no evidence that this notion is valid at the scale of slices of a few mm thickness. The Leverett J -function, used to calculate the local P_c curve is also well established for primary drainage at the scale of plugs belonging to the same rock-type, but there is no evidence that it can be used at the mm scale, and for imbibition. These two reasons can explain that this Leverett approach cannot reproduce the amplitude of the saturation profiles.

To reproduce the amplitude of saturation profiles, we need to introduce a different heterogeneity on the local P_c curve, not related to the local values of permeability and porosity but derived from the information given by the saturation profiles. For this purpose, we used the original Egermann approach that derives the local P_c from the calculation of the pressure profiles. The principle is an iteration process that first uses the pressures calculated on the equivalent homogeneous sample, and then uses the result to refine the determination of the local P_c curves. This method proved to be efficient for the Steady state experiment but not for the SDM one. Why?

The SS experiment shows that the sample is mixed wet with a large part of positive P_c curve. Due to procedure used in the SDM experiment, there is no information on the positive part of the P_c curve. This information should have been obtained with oil injection at decreasing flow rates. We understand that this procedure is difficult to realize experimentally since it implies change of injection procedure at $P_c=0$, and errors due to the dead volumes of fluids in the tubing. We prefer to recommend the procedure that is now considered as the state of the art for the determination of relative permeabilities: Steady state method followed by several bumps, the bumps are in fact similar to USS steps (Lenormand *et al.* [15]).

In this study, for the SS experiment, we obtained relative permeability curves very close whatever homogeneous or heterogeneous approaches were used to interpret the collected dataset. What could be the explanation? Difficult to give an answer, but this could be due to the non-local (long range averaging) of the pressures during flow in a porous medium, like for absolute permeability.

We have also performed the same interpretation for a Steady state displacement on a more heterogeneous whole core sample, but we cannot present the results due to confidentiality reasons. However, the results are similar: good fit with the saturation profiles using the

Egermann iteration process and final relative permeability similar to the homogeneous approach.

Even if the Kr curves are very close to the ones calculated with the homogeneous approach, we recommend performing this heterogeneous interpretation for all Kr experiments. We recognize that it takes around one additional hour for this interpretation, a short amount compared to the several weeks of months of experiments. With two advantages:

- 1) Better quality control: it is very satisfying to present a fit of the saturation profiles like in Figure 39 rather than the homogeneous one in Figure 29.
- 2) For the management of the uncertainties, the envelop of the Pc curves (Figure 38) is a very useful information for reservoir simulations (already pointed out by Egermann).

6 Conclusion

The purpose of this paper is to improve the numerical simulations of oil/water waterfloods used to determine the relative permeabilities. Even if the samples are as homogeneous as possible, the saturation profiles always present fluctuations. In this study we discuss the different methods to account for the various sources of heterogeneity in the simulation of the waterflood: porosity, permeability, and capillary pressure. The goal is to numerically reproduce the measured fluctuations of the saturation profiles.

We first describe the experiments: imbibition at reservoir conditions on 2 composite samples with similar plugs: a semi-dynamic method (close to Unsteady state) and a Steady state.

Then we describe several methods to account for heterogeneity: permeability profiles using Kozeny-Carman and Timur, and the original method from Egermann to derive Pc local curves from the saturation profiles.

The main result is that only the Egermann method is able to reproduce the experimental saturation profiles for the Steady state experiment. This result is an improvement for quality control of the simulation. However, for this experiment, the relative permeabilities determined by history matching are very close to the ones determined by the standard homogeneous approach.

This study leads to a general procedure to improve the simulations of relative permeability experiments.

References

1. Hicks, P.J. Jr., Deans, H.A., Narayanan, K.R.: "Distribution of Residual Oil in Heterogeneous Carbonate Cores Using X-ray CT", SPE Formation Evaluation, **03**, p. 235-240, SPE 20492, (1992).
2. Goggin, D., Thrasher, R., Lake, L.: "A theoretical and Experimental Analysis of Minipermeameter Response Including Gas Slippage and High Velocity Flow Effects", In-situ, **112**, p. 79-116, (1988)
3. Dauba, C., Hamon, G., Quintard, M., Cherblanc, F.: "Identification of parallel heterogeneities with miscible displacement", SCA-9933, 1999
4. Soltani, A., Le Ravalec-Dupin, M., Fourar, M., Egermann, P.: "A Non-Destructive Method for Characterization of One-Dimensional Permeability Distribution at the Core Scale", SCA2007-06, (2007).
5. Pairoys, F., Lasseux, D., Bertin, H.: "An Experimental and Numerical Investigation of Water-Oil Flow in Vugular Porous Media", SCA2003-20, (2003).
6. Hamon, G., Roy, C.: "Influence of Heterogeneity, Wettability and Coreflood Design on Relative Permeability Curves", SCA2000-23, (2000).
7. Ferreol, B.; Corre B.: "Determining Relative Permeabilities by Use of Experimental Design for very Heterogeneous Samples", ECMOR 97, (1997).
8. Sylte, A., Mannseth, T.: "Relative Permeability and Capillary Pressure: "Effects of rock heterogeneity", SCA-9808, (1998).
9. Pairoys, F., Caubit, C., Alexander, M., Ramos, J.: "Comparing Centrifuge, Steady state and Semi-dynamic Methods for Relative Permeability and Capillary Pressure Determination: New Insights", SCA2021-019, (2021).
10. Kozeny, J.: "Ueber Kapillare Leitung des Wasser sim Boden", Sitzungsber Akad. Wiss., (1927).
11. Carman, P.C.: "Fluid Flow through Granular Beds", Transactions, Institution of Chemical Engineers, (1937).
12. Timur, A.: "An Investigation of Permeability, Porosity and Residual Water Saturation Relationship for Sandstone Reservoirs", The Log Analyst, (1968).
13. Lombard, J.M., Egermann, P., Lenormand, R., Bekri, S., Hajizadeh, M., Hafez, H., Modavi, A., Kalam, M.Z.: "Heterogeneity Study through Representative Capillary Pressure Measurements – Impact on Reservoir Simulation and Field Predictions", SCA2004-32, (2004).
14. Egermann, P., Lenormand, R.: "A New Methodology to Evaluate the Impact of Localized Heterogeneity on Petrophysical Parameters (Kr, Pc) Applied to Carbonate Rocks", Petrophysics, **46**, p. 335-345, (2005).
15. Lenormand, R. and Lenormand, G.: "Recommended procedure for determination of relative permeabilities", SCA2016-004, (2016)